Soil stoichiometric characteristics and influencing factors in karst forests under microtopography and microhabitat scales

Yi Dang[1,2,6], Hua Zhou[2,3], Wenjun Zhao[1,2], Yingchun Cui[1,2], Chengjiang Tan[4], Fangjun Ding[1,2], Yukun Wang[5], Run Liu[2], Peng Wu[1,2]

[1]Guizhou Libo Karst Forest Ecosystem Observation and Research Station, Guizhou Academy of Forestry, Guiyang, 550005, China

[2]Key Laboratory of National Forestry and Grassland Administration on Biodiversity Conservation in Karst Mountainous Areas of Southwestern China, Guizhou Academy of Forestry, Guiyang, 550005, China

[3]Guizhou Liping Rocky Desertification Ecosystem Observation and Research Station, Guizhou Academy of Forestry, Guiyang, 550005, China

[4]Maolan National Nature Reserve Administration, Libo, 558400, China

[5]School of Soil and Water Conservation, Beijing Forestry University, Beijing, 100083, China.

[6]Guizhou Leigongshan Forest Ecosystem Observation and Research Station, Guizhou Academy of Forestry, Guiyang, 550005, China

Correspondence: Run Liu (18285115229@163.com) and Peng Wu (zuishaoxu@163.com)

Abstract. To quantitatively evaluate the stoichiometric characteristics of karst forest soils and their response mechanisms to complex microenvironments, this study systematically investigated the patterns of soil nutrients and influencing factors across different microtopography and microhabitat scales in the Maolan karst forest. The results indicated that: (1) The variability of soil nutrient contents in the study area was generally moderate or higher, indicating strong spatial heterogeneity. (2) Microhabitat factors (stone gully, stone surface, soil surface) significantly influenced nutrient accumulation, though different elements showed distinct response patterns to microhabitat variations. (3) Microtopographic factors (slope degree, slope aspect, slope position) were not only significantly correlated with soil nutrient patterns but also governed the spatial distribution gradients of certain nutrient elements. (4) Different response mechanisms of nutrients to microtopographic and microhabitat factors, combined with the different nutrient regulation and absorption strategies of various plant life forms (evergreen trees, deciduous trees, shrubs, herbs), collectively shaped the complex stoichiometric characteristics. The factors of microhabitat, microtopography, and plant life form exhibited synergistic effects on the soil stoichiometric characteristics in karst forests, with microhabitat and microtopographic factors playing a dominant role at this scale. Although biotic factors like plant life forms showed relatively weaker direct influences, their regulatory effects were closely interrelated with microhabitat and microtopographic factors. This multidimensional feedback mechanism reflects the complexity of nutrient cycling in karst soils.

Keywords. Karst; Microtopography; Microhabitat; Plant life form; Soil stoichiometry; Maolan National Nature Reserve

1 Introduction

Ecological stoichiometry, which integrates core theories from ecology, biology, chemistry, and other disciplines, is a science that studies the balance of energy and multiple chemical elements within biological systems. It focuses on how elemental balance regulates and influences ecological processes (e.g., growth, decomposition, and nutrient cycling), playing a crucial role in elucidating the coupling mechanisms between energy flow and elemental cycling in ecosystems (Chen et al., 2024). As a core component, soil stoichiometric characteristics serve not only as key indicators for assessing soil nutrient availability, microbial metabolic activity, and organic matter decomposition rates in fragile ecological regions but also as an important tool for understanding the coupling relationships of key soil nutrient elements in biogeochemical cycles and ecological processes (Joshi and Garkoti, 2023). Particularly in highly heterogeneous fragile ecosystems, the spatial variation of soil stoichiometric characteristics can act as a latent factor driving vegetation pattern succession (Chen et al., 2022). Therefore, analyzing soil stoichiometric characteristics and their driving mechanisms is a critical approach to understanding ecosystem functioning and vulnerability management (An et al., 2019). The related theoretical framework integrates the elemental allocation patterns across the soil-plant-microbe continuum into a unified dimension, providing a quantitative tool for understanding resource limitations and ecosystem stability (Sardans et al., 2021), and holds key significance for revealing environmental stress and ecological restoration potential in fragile ecological regions (Zhang et al., 2024).

China's karst region is renowned for its significant ecological fragility and habitat heterogeneity, covering a total area of approximately 1.3 million km², which accounts for 13.5% of the country's land area (Wu et al., 2025). The Maolan karst area, a typical karst ecosystem in southwestern China, features soils primarily derived from carbonate rocks. These soils are characterized by slow pedogenesis, shallow depth, and severe exposure of shallow bedrock (Tang et al., 2019). Influenced by soil erosion and karst processes, the area is fragmented into complex and heterogeneous microhabitats (Tang et al., 2019). The formation of microhabitat heterogeneity itself is closely linked to pronounced topographic factors and distinctive vegetation patterns. Consequently, this complex assemblage, which differs markedly from normal landforms, reshapes the spatial distribution patterns of soil moisture and nutrients in karst areas, resulting in an "island-like" heterogeneous distribution pattern. This heterogeneity not only exacerbates the decoupling of major nutrient element cycles in soils but may also compel the plant-soil system to adjust through stoichiometric homeostasis to adapt to resource limitations (Zhang et al., 2022). Previous studies have indicated that at regional scales, climatic conditions and soil parent material are the dominant factors determining the distribution patterns of soil nutrients. However, at landscape and finer scales, the key drivers shaping the heterogeneity of soil stoichiometric characteristics are often closely associated with specific azonal factors, such as topography, habitat features, and vegetation types. Although numerous studies have explored the stoichiometric characteristics of major elements like soil carbon (C), nitrogen (N), and phosphorus (P) at global or regional scales, research on soil nutrient distribution patterns and their controlling factors in karst regions, particularly at the slope scale, remains limited (Feng et al., 2024). Understanding of how soil stoichiometric characteristics respond to microtopography, microhabitats, and vegetation is still inadequate. This knowledge gap somewhat constrains our comprehension of the synergistic evolution mechanisms between soil and vegetation in karst ecosystems. To address this gap, our study focuses on the Maolan karst area. By systematically collecting soil samples under different microhabitat and microtopographic conditions, combined with survey data on surface plant life forms, we aim to determine soil stoichiometric characteristics and specifically address the following scientific questions:

1) What are the spatial distribution patterns and heterogeneity of major soil nutrient contents and stoichiometric characteristics in the karst area?

2) What are the interrelationships among soil nutrient elements, and what is the intrinsic regulatory mechanism governing their stoichiometric balance?

3) What are the relative contributions of microhabitat types, microtopographic features, and vegetation life forms to soil stoichiometric characteristics, and how do these factors interact with each other?

Through a comprehensive multivariate analysis, this study aims to elucidate the underlying mechanisms shaping the stoichiometric characteristics of karst soils. The findings will provide a novel theoretical basis for understanding the coupled soil-vegetation adaptation mechanisms in karst ecosystems, thereby offering scientific support for ecological restoration and sustainable management in this region.

2 Study area and methods

2.1 Study area

The study area is located within the Maolan National Nature Reserve in Guizhou Province, situated in the transitional slope zone from the Yunnan-Guizhou Plateau to the northern Guangxi hills. Its geographical coordinates range from 107°52'10"to 108°05'40"E and 25°09'20" to 25°20'50"N. The topography exhibits a distinct northwest-high, southeast-low pattern, with elevations ranging from 430.0 to 1078.6 m (predominantly 550-850 m) (Zhou et al., 2022). This region features a typical mid-subtropical monsoon humid climate, with meteorological data indicating: an annual average temperature of 15.3°C (coldest month: 5.2°C; warmest month: 23.5°C), annual precipitation of 1,752.5 mm (concentrated in summer), annual relative humidity of 83.0%, annual sunshine duration of 1,272.8 h, frost-free period of 315 d, and total annual solar radiation of 63.29 $kW\cdot m^{-2}$ (Wen and Jin, 2019).

The geological structure is predominantly composed of limestone and dolomite, forming a typical bare karst peak-cluster depression system with bedrock exposure exceeding 80.0%. Soil resources exhibit pronounced spatial constraints, primarily distributed in rock fissures with shallow and discontinuous profiles. Chemically, soils are characterized by high calcium content, base cation enrichment, and elevated organic matter, classified mainly as black limestone soils. The vegetation comprises primary karst evergreen-deciduous broadleaved mixed forests, representing azonal vegetation, with a forest coverage rate of 87.4%. This ecosystem stands as the best-preserved and most representative karst forest ecosystem at the same latitude in the Northern Hemisphere (Zhou et al., 2022).

2.2 Plot setting

As complete random sampling was impractical in the study area due to its status as a national nature reserve and the highly fragmented karst habitats, this study primarily employed a stratified random sampling method to establish sampling points. The specific procedure was as follows: based on a systematic investigation of existing fixed plots at the Libo Karst Forest Ecosystem Positioning Observation Research Station, a predefined stratification was conducted across five habitat strata: microhabitat, plant life form, slope degree, slope aspect, and slope position. Within each of these combination units (e.g., sharp slope + semi-shady slope + downslope + stone gully + evergreen trees), random grids were generated. After field reconnaissance to verify the feasibility of these points and eliminate unsuitable locations, alternative points were manually identified within the same stratum. Finally, the setup of all sampling points was completed. During the field investigation, geographic coordinates (latitude and longitude) and elevation data for each sample tree were recorded using high-precision handheld GPS devices. The slope aspect and slope degree of the plots were measured with professional compasses. Slope position and microhabitat information were determined through on-site observation (Figure 1). The number of plots corresponding to each classification stratum is detailed in the supplementary material (Table S1).

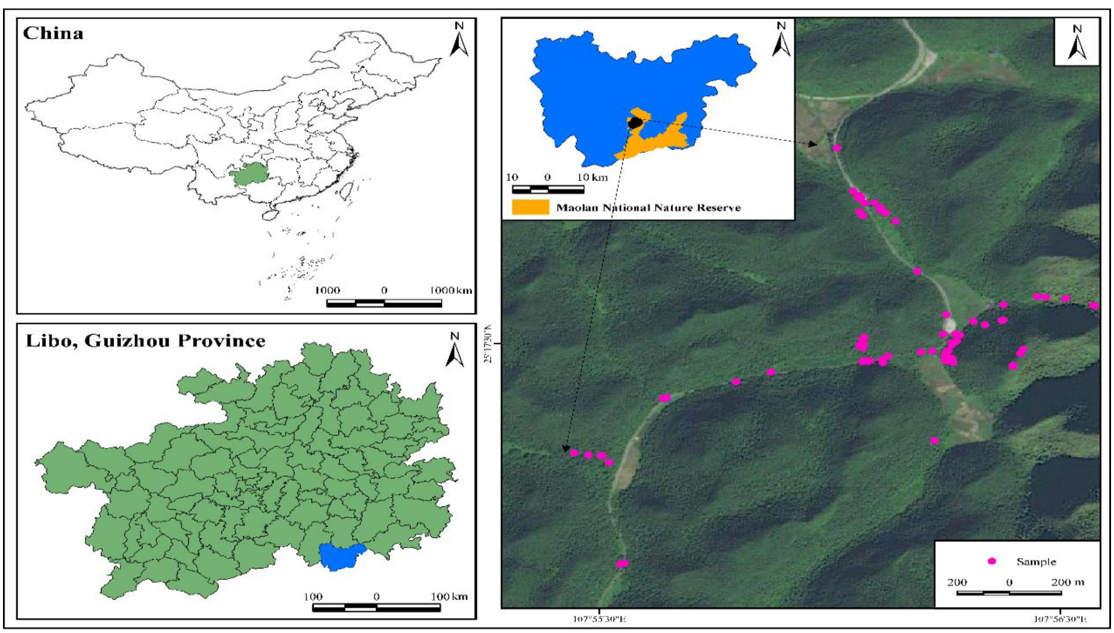

Figure 1. Spatial distribution maps of sampling sites in Maolan National Nature Reserve, Libo, Guizhou. Four-tier geolocation hierarchy: China's national framework (top-left) with green area indicating Guizhou Province; Libo County boundaries (bottom-left) with blue zone marking study townships; Maolan National Nature Reserve (top-right) with orange area delineating protected core zone; Satellite imagery of sampling sites (bottom-right) with pink circles designating soil sampling locations. (Scale bars: 1000 km/100 km/10 km/200 m; north arrows: N)

2.3 Microtopography division

The microtopographic features of the study area can be systematically classified according to the following scheme (Wu et al., 2025):

Slope position: upslope, midslope, downslope, and depression (four classes);

Slope degree: flat slope (≤ 5°), gentle slope (5 - 15°), tilted slope (15 - 25°), steep slope (25 - 35°), and sharp slope (≥ 35°) (five classes);

Slope aspect: shady slope (337.5-22.5°, 22.5-67.5°), semi-shady slope (67.5-112.5°, 292.5-337.5°), flat land, semi-sunny slope (112.5-157.5°, 247.5-292.5°), and sunny slope (157.5-247.5°) (five classes).

2.4 Microhabitat division

Microhabitat refers to the micro-scale environmental units where individual organisms or populations reside, characterized by local topography, substrate type, and microclimate. While no universally accepted definition exists regarding its spatial scale, this study adopts a karst forest microhabitat classification system established in prior research. Practically, microhabitats in the study area were categorized into three types—stone surface, stone gully, and soil surface—based on principles of representativeness, distinctiveness, and operational feasibility (Wu et al., 2025). The specific classification criteria are as follows:

The stone surface microhabitat refers to microenvironmental units where bedrock is directly exposed at the surface. Identification criteria require fulfillment of any of the following conditions: Bedrock exposure rate > 50.0%, with solution gully depth > 30 cm and surface soil cover area < 1 m²; or development of shallow dissolution micro-landforms including shallow stone gullies, small rock troughs, shallow solution pits, and narrow rock crevices, all with vertical dimensions ≤ 30 cm; or stone surfaces with soil cover area < 1 m² and thickness < 20 cm.

The stone gully microhabitat refers to gully-shaped microenvironmental units formed through karst erosion processes. Identification criteria require fulfillment of any of the following conditions: bedrock exposure rate > 50.0% with gully depth > 30 cm and soil cover area < 1 m²; gully depth < 30 cm but soil layer thickness > 20 cm; or bedrock exposure rate < 50.0% but presence of soil-dominated gullies with depth > 30 cm.

The soil surface microhabitat refers to microenvironmental units with continuous and homogeneous soil coverage and relatively well-developed soil horizons. Identification criteria require fulfillment of either of the following conditions: continuous soil cover with an area ≥ 1 m², or soil cover area < 1 m² with bedrock exposure rate ≤ 50.0% and absence of gullies deeper than 30 cm.

2.5 Soil sample collection and determination

Due to the typical karst terrain of the study area, characterized by an extremely thin surface soil layer, samplers completed soil collection using only a shovel and cutting rings (100 cm³), without requiring tools like soil augers designed for deep soil sampling. Upon reaching a sampling point, the area within a 20 cm radius of plant root distribution was selected. After removing surface litter, three intact soil cores were collected using cutting rings. Following the manual removal of non-soil materials, the samples were thoroughly mixed, ensuring a net weight of ≥ 500 g per sample. The samples were immediately coded, sealed in sterile sampling bags, and temporarily stored in a portable cooler for subsequent analysis.

Samples were processed in batches upon returning to the laboratory. For the determination of pH, hydrolyzable nitrogen (HN), available phosphorus (AP), available potassium (AK), exchangeable calcium (ExCa), and exchangeable magnesium (ExMg), the soil samples were passed through a 2-mm nylon sieve. This procedure preserved the intact soil structure, avoided the destruction of active components through grinding, and ensured that the extraction of readily available nutrients reflected true field conditions. For the determination of soil organic carbon (SOC), total nitrogen (TN), total phosphorus (TP), total potassium (TK), total calcium (TCa), and total magnesium (TMg), the soil samples were passed through a 0.149-mm sieve(Table 1). All residual material not passing the 0.149 mm sieve was subjected to secondary grinding using an agate mortar until it completely passed through. This portion was then thoroughly mixed with the sieved fine soil fraction to form an analytical sample representing the entirety of the original soil matrix (after removal of > 2 mm gravel). This approach ensures thorough sample homogenization, eliminating interference from particle size effects on total elemental analysis and guaranteeing the completeness of digestion/fusion. Furthermore, it allows for the inclusion of elements from all soil components in the analysis, preventing deviation of measurement results from true values due to the discarding of any fraction, thereby ensuring the accuracy and representativeness of the data.

Soil sample preparation strictly adhered to the *Chinese Forestry Industry Standard LY/T 1210-1999*. Analytical protocols included: pH determination via potentiometric method; soil organic carbon (SOC) quantified by potassium dichromate oxidation-external heating; total nitrogen (TN) via semi-micro Kjeldahl digestion; hydrolyzable nitrogen (HN) by alkali-hydrolyzable diffusion; total phosphorus (TP) using alkaline fusion-molybdenum-antimony-ascorbic acid spectrophotometry; available phosphorus (AP) extracted by hydrochloric–sulfuric acid leaching method; total potassium (TK) measured through alkaline fusion-flame photometry; available potassium (AK) extracted with ammonium acetate extraction - flame photometry; total calcium (TCa) and total magnesium (TMg) determined by atomic absorption spectrophotometry (AAS); exchangeable calcium (ExCa) and magnesium (ExMg) analyzed via ammonium acetate exchange-AAS method. All analyses strictly adhered to the specifications of the *Chinese Forestry Industry Standards (LY/T 1210-1999)* and were performed using air-dried soil samples. During sample processing, the air-drying procedure was conducted promptly and consistently, with soil samples stored in a cool, dry place to minimize any potential effects associated with the air-drying process. Pretreatment and analytical conditions were maintained consistent for all samples to ensure data comparability and reliability. (Table 1) (Yang and Da, 2006).

Table 1. Analytical methods and core instrumentation for determining soil properties.

Detection Indicator	Standard Method	Core Instrumentation
pH	Potentiometric method	pH meter (accuracy ±0.01)
SOC	Potassium dichromate oxidation - external heating method	Oil bath (180°C ±0.5°C), Titration apparatus
TN	Semi-micro Kjeldahl method	Kjeldahl nitrogen analyzer, Digestion block/furnace
HN	Alkaline hydrolysis - diffusion method	Constant temperature incubator, Diffusion dish
TP	Alkaline fusion-molybdenum-antimony-ascorbic acid spectrophotometry	Muffle furnace, Spectrophotometer
AP	Hydrochloric–sulfuric acid leaching method	Oscillator/shaker, Spectrophotometer
TK	Alkali fusion - flame photometry	Muffle furnace, Flame photometer
AK	Ammonium acetate extraction - flame photometry	Centrifuge, Flame photometer
TCa & TMg	Atomic absorption spectrophotometry	Atomic Absorption Spectrometer (AAS)
ExCa & ExMg	Ammonium acetate exchange - AAS method	Centrifuge, Atomic Absorption Spectrometer (AAS)

2.6 Vegetation survey and plant nutrient analysis

During soil sample collection, field personnel simultaneously recorded the plant species and life forms at each sampling point and collected representative leaf samples. Plant species were identified to the species level using taxonomic methods, and their Latin names were documented. Plant life forms were classified into four categories—evergreen trees, deciduous trees, shrubs, and herbs—based on standard botanical criteria and adapted to the local conditions of the study area. Leaf sampling followed the principle of representativeness: using high-pruners, well-developed branches from the east, south, west, north, upper, middle, and lower parts of the canopy were clipped. Fully expanded, disease-free, intact leaves without petioles were then picked from these branches. The collected leaves were thoroughly mixed, and a subsample of 30–50 leaves was retained using the quartering method. These samples were labeled, sealed in zip-lock bags, and stored in a portable refrigerator for subsequent analysis.

The preparation of plant samples referred to the industry standard LY/T 1267–1999. Carbon (C) content was determined by the potassium dichromate oxidation–external heating method; nitrogen (N) content by the Kjeldahl method; phosphorus (P) content by the molybdenum–antimony anti-spectrophotometric method; potassium (K) content by flame photometry; and calcium (Ca) and magnesium (Mg) contents by atomic absorption spectrophotometry(Table 2). All analytical procedures were strictly conducted in accordance with the *Chinese Forestry Industry Standards (LY/T 1210–1275-1999)* (Yang and Da, 2006).

Table 2. Analytical methods and core instrumentation for determining plant properties.

Detection Indicator	Standard Method	Core Instrumentation

C	Potassium dichromate oxidation–external heating method	Oil bath (180°C ± 0.5°C), Titration apparatus
N	Kjeldahl method	Kjeldahl nitrogen apparatus, Digestion furnace
P	Molybdenum–antimony anti-spectrophotometric method	Muffle furnace, Spectrophotometer
K	Flame photometry	Muffle furnace, Flame photometer
Ca & Mg	Atomic absorption spectrophotometry	Atomic absorption spectrometer (AAS)

2.7 Data processing and analysis

This study used mass contents to characterize soil nutrient indicators (SOC, TN, TP, etc., totaling 11 items; see supplementary material Table S2 for details). The stoichiometric ratios of the elements were calculated as mass ratios (SOC:TN, SOC:TP, SOC:TK, etc., totaling 9 items; see supplementary material Table S3 for details). Data analysis was performed using SPSS 25.0 and Excel 2016 for statistical processing, and graphical outputs were generated via Origin 2021. The Kolmogorov-Smirnov (K-S) test was applied to assess data normality. Prior to correlation analysis, raw data were logarithmically transformed [ln(x+1)] to meet ANOVA assumptions and normality requirements. Homogeneity of variance was tested before conducting ANOVA, with LSD or Tamhane's T2 methods selected for multiple comparisons based on test outcomes (Nagamatsu et al., 2003). For associations between soil stoichiometric characteristics (continuous variables) and numerically coded environmental factors (ordinal variables), this study employed Spearman's rank correlation for determination. The coefficient of variation is denoted as CV in this study, and the criteria for classifying its variation intensity are as follows: weak ($CV \leq 0.20$), moderate ($0.20 < CV < 0.50$), and strong ($CV \geq 0.50$) (Han et al., 2019).

This study employed redundancy analysis (RDA) using CANOCO 5.0 software to examine the relationships between soil stoichiometric characteristics and environmental factors. Environmental variables were coded as follows: slope positions (upslope, midslope, downslope, depression) were assigned values 1–4; slope degrees (flat, gentle, tilted, steep, sharp) were assigned 1–5; slope aspects (shady, semi-shady, flat land, semi-sunny, sunny) were assigned 1–5; microhabitats (soil surface, stone gully, stone surface) were assigned 1–3; and life forms (evergreen trees, deciduous trees, shrubs, herbs) were assigned 1–4. Monte Carlo permutation tests were applied to assess the significance of the constrained ordination model and to quantify the influence of individual environmental factors on soil stoichiometric characteristics. Variance partitioning analysis (VPA) was performed using the vegan package in R 4.4.1 to determine the explanatory contributions of different categories of environmental factors and their interactions. The influencing factors included three groups: (i) microenvironmental factors (slope degree, slope aspect, slope position, microhabitat), (ii) plant structural factors (plant species, life forms), and (iii) plant nutrient factors (plant nutrient contents: C, N, P, K, Ca, Mg). Soil stoichiometric characteristics served as response variables, encompassing all 11 soil nutrient contents and 9 stoichiometric ratios. The adjusted R^2 value was used to evaluate the goodness-of-fit of the model.

3 Results and Analysis

3.1 Stoichiometric characteristics of soil in the Maolan Karst region

Soil nutrient contents in the study area generally exhibited strong spatial variability. Kolmogorov-Smirnov (K-S) tests indicated that only total phosphorus (TP) and total potassium (TK) followed a normal distribution ($P > 0.05$), while the majority of other nutrients deviated from normality. Analysis based on the coefficient of variation (CV) revealed high variability for most nutrients, particularly for available phosphorus (AP) (CV = 0.95). In contrast, only TP, TK, and total magnesium (TMg) showed moderate variability (CV ≤ 0.50). The spatial patterns suggested that the maximum values of soil pH and nutrient contents were frequently associated with stone surfaces and downslope positions, whereas the minimum values were often found on soil surface microhabitats and midslope positions. These patterns preliminarily highlight the significant influence of microtopography and microhabitat on nutrient spatial distribution. (Detailed descriptive statistics are provided in supplementary material Tables S2 and S3.

3.1.1 Soil stoichiometric characteristics across different slope degrees

Soil nutrients and their stoichiometric ratios exhibited distinct distribution trends across different slope degrees. Statistical analysis (Table S4) revealed that the mean values of most nutrient contents were highest on flat slopes and lowest on sharp and steep slopes, with significant differences observed between the maximum and minimum values for certain elements. For example, the difference in TP between flat slopes and sharp slopes was highly significant (MD = 0.222, 95% CI [0.058, 0.385], $P = 0.009$). Only a few elements, such as TMg, displayed an opposite trend, with the highest enrichment observed on sharp slopes. The highest mean stoichiometric ratios were almost all concentrated on sharp and steep slopes, while the lowest means were mainly scattered across slope types other than flat slopes, with a relatively high frequency on tilted slopes. However, the distribution trend of TCa:TMg differed from the others, being highest on flat slopes and lowest on gentle slopes. Although the former was 1.54-fold higher than the latter, the difference was not significant (MD = 0.234, 95% CI [−0.119, 0.587], $P = 0.19$) (Figure 2).

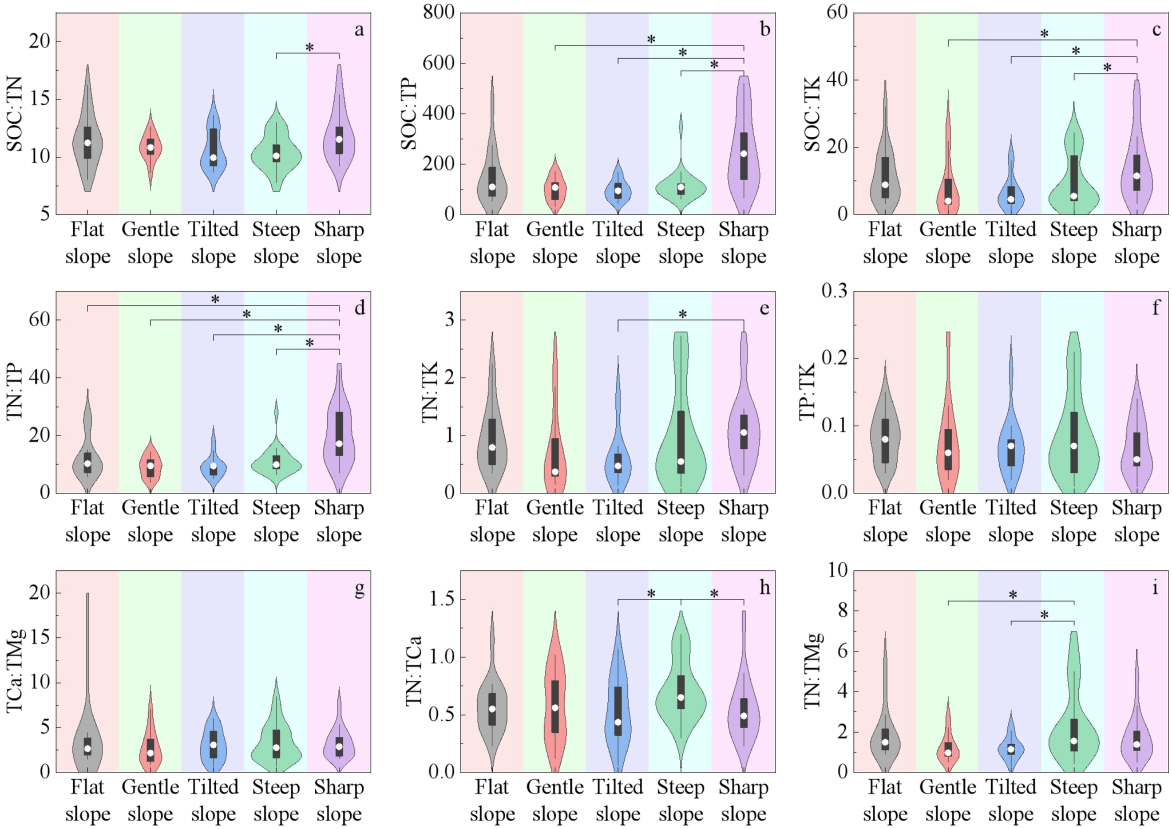

Figure 2. Distribution differences in stoichiometric ratios of major soil nutrients across different slope degree types, presented as violin plots overlaid with box plots. The Y-axis of each subplot denotes the values of corresponding ratios, while the X-axis represents slope degree types. An asterisk (*) indicates significant intergroup differences ($P < 0.05$), with black horizontal lines connecting groups exhibiting differences. The number of samples (n) for each slope degree type is as follows: flat slope (n = 16), gentle slope (n = 12), tilted slope (n = 14), steep slope (n = 27), sharp slope (n = 17).

3.1.2 Soil stoichiometric characteristics across different slope aspects

Major soil nutrients were highest on flat land, followed by shady slopes, and lowest on sunny slopes. Statistical analysis (Table S5) showed that the minimum mean values of most elements were predominantly concentrated on sunny slopes and semi-sunny slopes, while the maximum mean values occurred more frequently on flat land, shady slopes, or semi-shady slopes. The differences between these extremes were often significant. For example, the difference in SOC between semi-shady slopes and sunny slopes was highly significant (MD = 0.501, 95% CI [0.141, 0.860], $P = 0.007$). However, the distribution trends of a very few elements were exceptional; for example, TK content was highest on sunny slopes, but the differences among all slope aspects were not significant. Due to the uneven distribution of elemental contents across slope aspects, the minimum mean values of stoichiometric ratios were mainly found on sunny slopes and similar areas, while the maximum means were scattered without a clear trend. In general, most elemental stoichiometric ratios were relatively similar across different slope aspects. Only a few, such as SOC:TK, reached significant differences between aspects like semi-shady slopes and sunny slopes (MD = 0.462, 95% CI [0.054, 0.870], $P = 0.027$) (Figure 3).

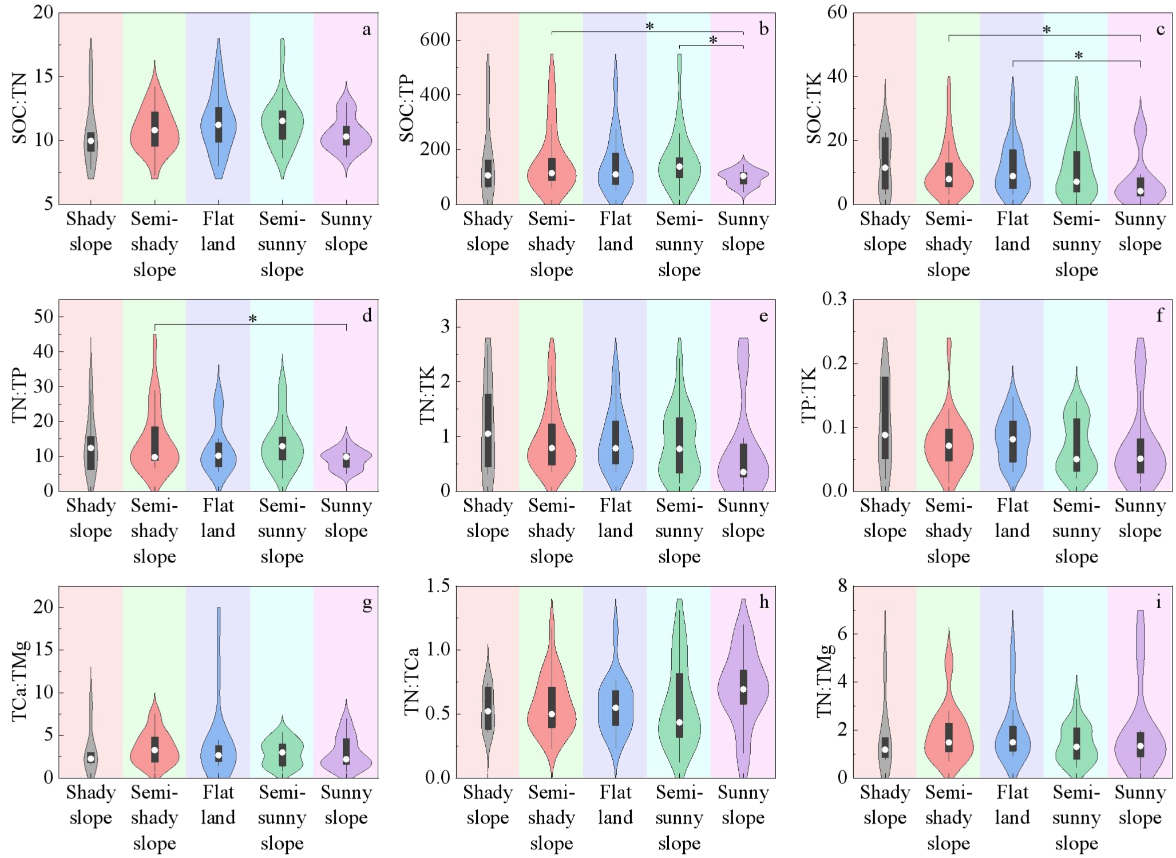

Figure 3. Distribution differences in stoichiometric ratios of major soil nutrients across different slope aspect types, presented as violin plots overlaid with box plots. The Y-axis of each subplot denotes the values of corresponding ratios, while the X-axis represents slope aspect types. An asterisk (*) indicates significant intergroup differences ($P < 0.05$), with black horizontal lines connecting groups exhibiting differences. The number of samples (n) for each slope aspect type is as follows: shady slope (n = 6), semi-shady slope (n = 22), flat land (n = 16), semi-sunny slope (n = 19), sunny slope (n = 23).

3.1.3 Soil stoichiometric characteristics across different slope positions

Soil primary nutrients and their stoichiometric ratios exhibited distinct distribution patterns across different slope positions. Statistical analysis (Table S6) showed that the mean content of most nutrients was highest at the upslope position and lowest at the midslope position, with significant differences often observed between these two positions. For example, the difference in TN between the upslope and midslope positions was highly significant (MD = 0.735, 95% CI [0.294, 1.176], $P = 0.001$). Due to the relatively higher contents of SOC and TN at the upslope position, the maximum values of their related stoichiometric ratios (e.g., SOC:TN, TN:TP) were also primarily distributed at the upslope position. Constrained by the distribution of element contents across slope positions, the various stoichiometric ratios were relatively similar between the downslope position and depression, with almost no significant differences observed. In contrast, significant differences existed for nearly all ratios between the midslope and downslope positions, except for TN:TCa. Among these, the mean difference in SOC:TN between the midslope and downslope positions was even highly significant (MD = 0.112, 95% CI [0.038, 0.186], $P = 0.004$) (Figure 4).

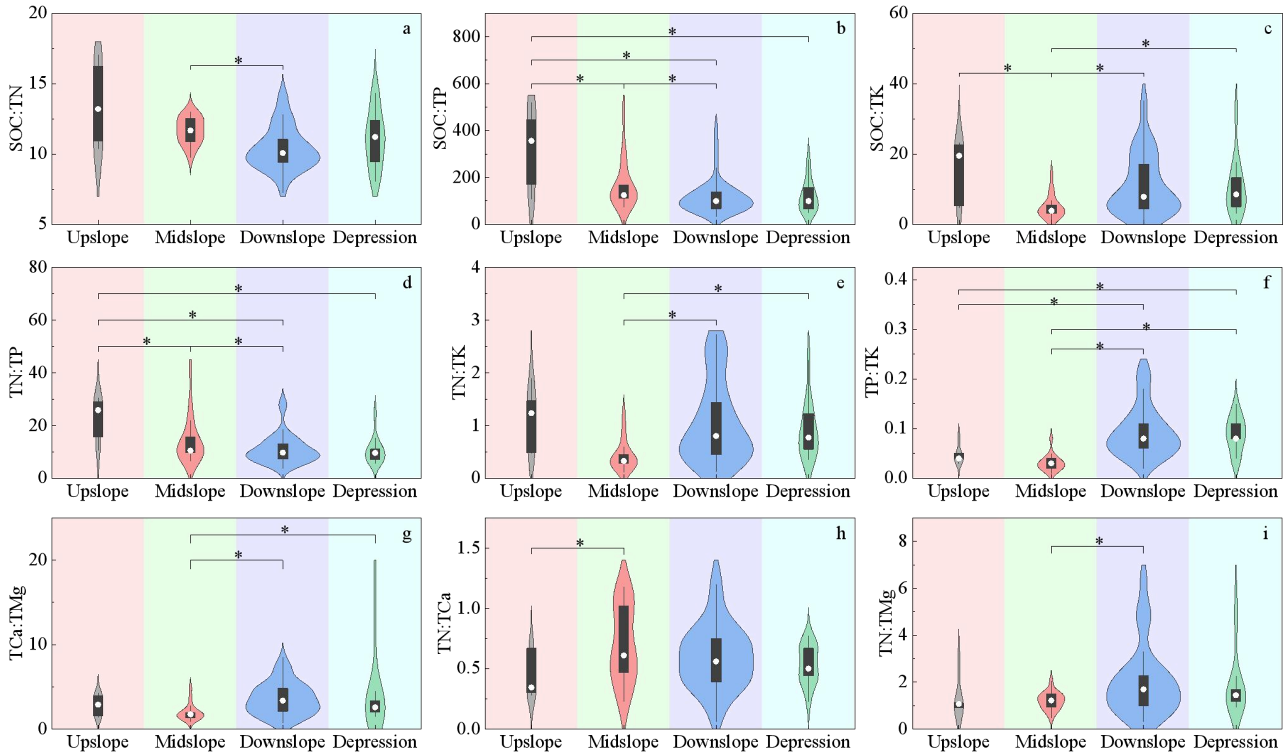

Figure 4. Distribution differences in stoichiometric ratios of major soil nutrients across different slope position types, presented as violin plots overlaid with box plots. The Y-axis of each subplot denotes the values of corresponding ratios, while the X-axis represents slope position types. An asterisk (*) indicates significant intergroup differences ($P < 0.05$), with black horizontal lines connecting groups exhibiting differences. The number of samples (n) for each slope position type is as follows: upslope (n = 6), midslope (n = 18), downslope (n = 49), depression (n = 13).

3.1.4 Soil stoichiometric characteristics across different microhabitats

The distribution of major soil nutrients across the three microhabitats generally followed similar trends: both elemental contents and stoichiometric ratios tended to be lower on the soil surface and higher on the stone surface, with significant differences often observed between these two microhabitats. Values in the stone gully generally fell between the other two. Statistical analysis (Table S7) indicated that carbon and nitrogen were more enriched in the stone surface microhabitat compared to other elements. Consequently, the maximum mean values of major nutrient stoichiometric ratios (e.g., SOC:TP, SOC:TK, TN:TP, TN:TK) were significantly greater in the stone surface microhabitat than in the soil surface microhabitat.

However, influenced by the distribution pattern of TCa, the trend for TN:TCa was opposite to the general pattern, with its mean value highest in the soil surface microhabitat and lowest in the stone surface microhabitat. The value in the soil surface microhabitat was 1.29 times that in the stone surface microhabitat, and the difference was significant (MD = 0.091, 95% CI [0.006, 0.177], $P = 0.004$) (Figure 5).

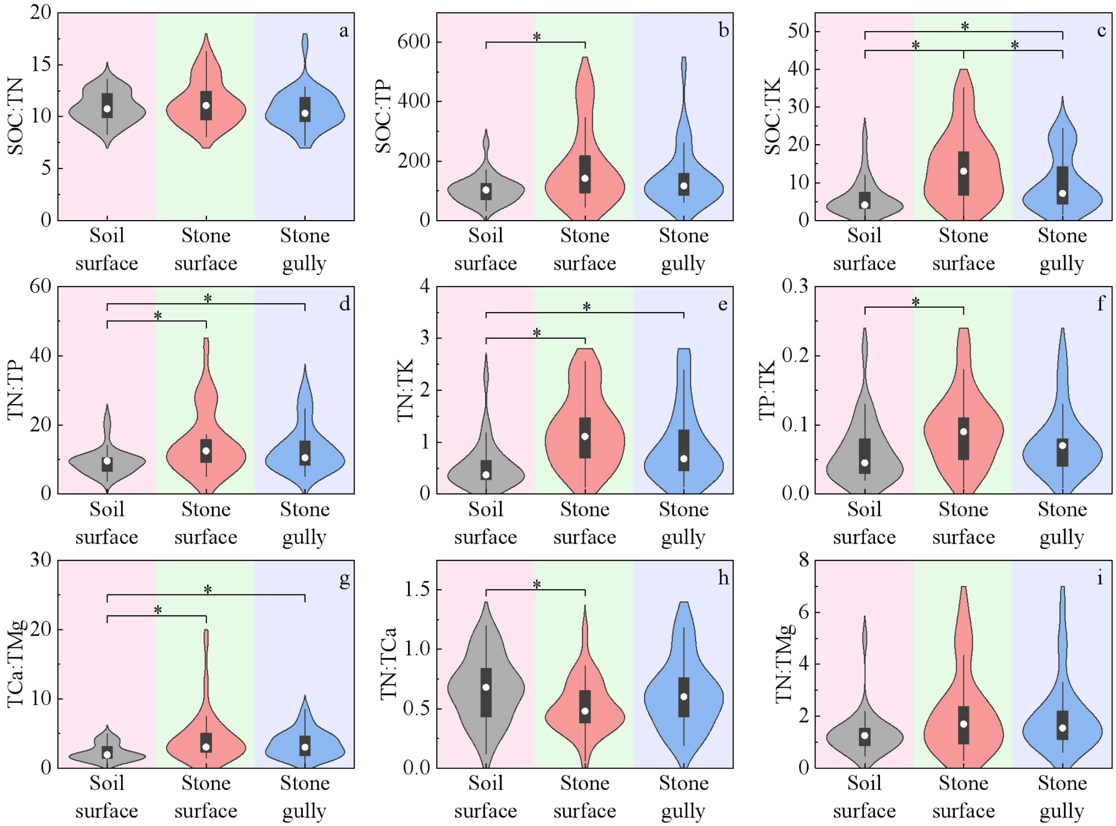

Figure 5. Distribution differences in stoichiometric ratios of major soil nutrients across different microhabitats, presented as violin plots overlaid with box plots. The Y-axis of each subplot denotes the values of corresponding ratios, while the X-axis represents microhabitats. An asterisk (*) indicates significant intergroup differences ($P < 0.05$), with black horizontal lines connecting groups exhibiting differences. The number of samples (n) for each microhabitat type is as follows: soil surface (n = 28), stone gully (n = 29), stone surface (n = 29).

3.1.5 Soil stoichiometric characteristics across different life forms

The distribution trends of most nutrients were similar in the rhizosphere soils of the four plant life forms. Statistical analysis (Table S8) indicated that the mean values of element contents and stoichiometric ratios were generally highest in herb soils and lowest in evergreen or deciduous tree soils, with the differences often being significant. Among these, the difference in TP between herb and evergreen tree soils was even highly significant (MD = 0.214, 95% CI [0.063, 0.365], $P = 0.006$). However, the distribution pattern of some elements, such as TK, was opposite to that of most elements, showing significantly higher values in trees than in shrubs and herbs. This regular distribution of element contents resulted in corresponding patterns for the major nutrient stoichiometric ratios. Higher values were mostly concentrated in the herb life form, while lower values occurred more frequently in deciduous tree soils. For example, the stoichiometric ratios TN:TK and TP:TK were influenced not only by the aforementioned distribution trend of TK but also by the fact that elements like TN and TP were present in greater, or significantly greater, quantities in herb soils compared to deciduous tree soils (Figure 6).

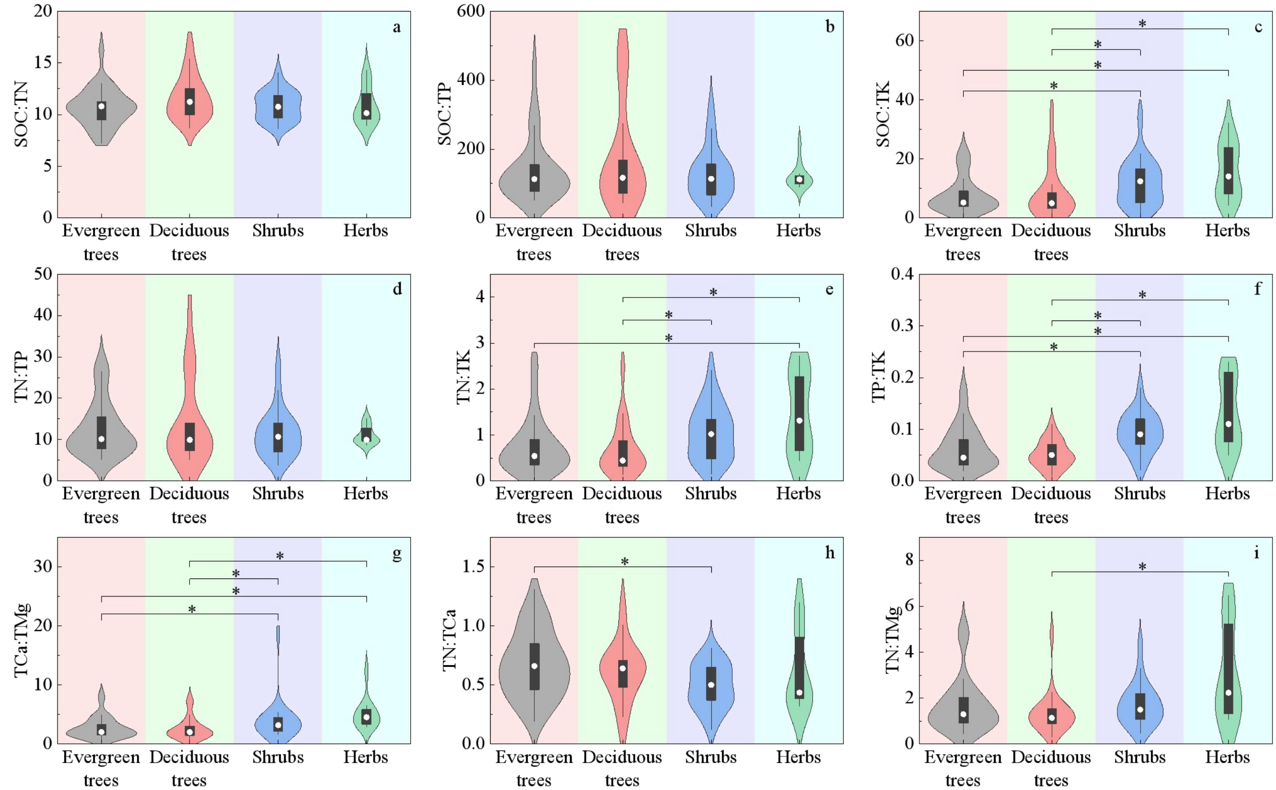

Figure 6. Distribution differences in stoichiometric ratios of major soil nutrients within the rhizosphere zones of different plant life forms, presented as violin plots overlaid with box plots. The Y-axis of each subplot denotes the values of corresponding ratios, while the X-axis represents plant life forms. An asterisk (*) indicates significant intergroup differences ($P < 0.05$), with black horizontal lines connecting groups exhibiting differences. The number of samples (n) for each plant life form is as follows: evergreen trees (n = 32), deciduous trees (n = 21), shrubs (n = 21), herbs (n = 12).

3.2 Correlation analysis between soil nutrient contents and stoichiometric ratios in karst regions

The correlation matrix revealed complex interrelationships among soil nutrients and their stoichiometric characteristics (Figure S1). Soil SOC and TN contents exhibited a strong co-variation trend (r = 0.94, $P < 0.01$), and both showed significant positive correlations with most other nutrients (e.g., HN, TCa, and ExCa). In contrast, TK content was significantly negatively correlated with SOC, TN, and several key stoichiometric ratios (e.g., SOC:TP, TN:TMg). Available phosphorus (AP) demonstrated a more independent pattern, showing significant positive correlations only with TCa and SOC.

Close associations were also observed among different stoichiometric ratios; for instance, SOC:TK and TN:TK exhibited a highly significant positive correlation (r = 0.95, $P < 0.01$). These association patterns indicate tightly coupled relationships among major nutrient elements such as carbon, nitrogen, and calcium, as well as the unique distribution pattern of certain individual elements within the karst soil system. The underlying driving mechanisms will be thoroughly analyzed in the Discussion section.

3.3 Influencing factors of soil stoichiometric characteristics in karst regions

To investigate the effects of factors including microtopography, microhabitat, and plant life forms on soil stoichiometric characteristics, this study performed Redundancy Analysis (RDA; Figure 7) and correlation analysis (Table S9). The results indicated that the first two RDA axes cumulatively explained 23.1% of the relationship between the soil stoichiometric variables and the environmental factors (microtopography, microhabitat, plant life forms). Monte Carlo permutation tests revealed that microhabitat was the most significant factor influencing the soil stoichiometric characteristics ($P < 0.01$), uniquely explaining 10.4% of the variance. It was followed by slope position (8.0%), plant life forms (5.3%), and slope aspect (1.8%). In contrast, the effect of slope degree was not statistically significant ($P = 0.15$), exhibiting the lowest explanation rate (1.4%) and contribution rate (5.6%) (Table 3). Spearman's rank correlation analysis (Table S9) further supported the RDA results: 90% of the soil stoichiometric indicators showed significant or highly significant correlations with microhabitat, whereas the proportion of indicators significantly correlated with other factors ranged from 30% to 70%. The RDA biplot (Figure 7) clearly illustrated that microhabitat was positively correlated with most soil nutrient contents and their stoichiometric ratios (e.g., TCa, TN, SOC:TK) and was negatively correlated with only a few indicators (e.g., TK, TN:TCa).

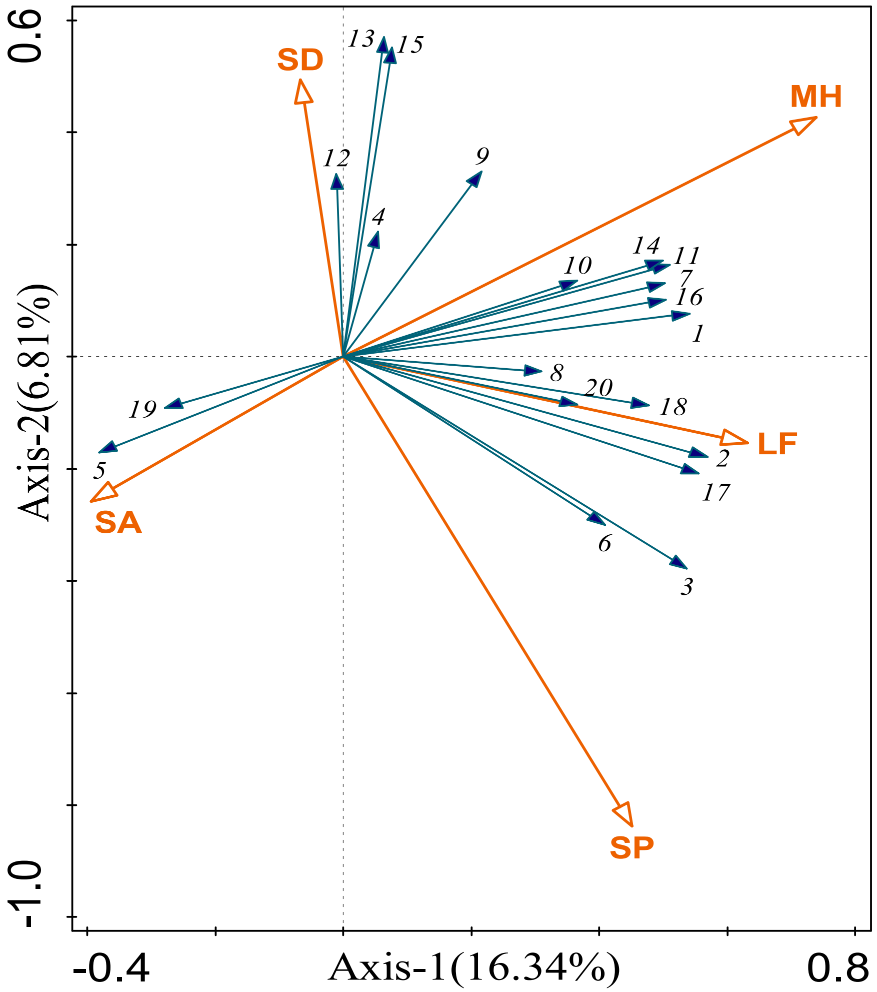

Figure 7. Ordination biplot of redundancy analysis (RDA) for soil stoichiometric characteristics and environmental factors. Axes: RDA1 (16.3% variance explained) and RDA2 (6.8%). Blue arrows represent stoichiometric variables: 1(TN), 2(HN), 3(TP), 4(AP), 5(TK), 6(AK), 7(TCa), 8(ExCa), 9(TMg), 10(ExMg), 11(SOC), 12(SOC:TN), 13(SOC:TP), 14(SOC:TK), 15(TN:TP), 16(TN:TK), 17(TP:TK), 18(TCa:TMg), 19(TN:TCa), 20(TN:TMg). Red arrows represent environmental variables: MH (Microhabitat), SP (Slope Position), SA (Slope Aspect), SD (Slope Degree), LF (Life Form). Arrow length denotes variable contribution; inter-arrow angles reflect correlations. Origin (0,0) serves as the reference point.

Table 3. Results of Monte Carlo test of effects of environmental factors on Soil stoichiometric characteristics.

Environmental factor	Explains rate/%	Contribution rate/%	*F* value	*P* value
Microhabitat	10.4	40.7	10.8	0.00
Slope position	8.0	27.1	7.8	0.00
Life forms	5.3	18.8	5.7	0.00
Slope aspect	1.8	7.9	2.4	0.02
Slope degree	1.4	5.6	1.7	0.09

To comprehensively quantify the contributions of different factor categories to soil stoichiometric characteristics, this study performed variance partitioning analysis (VPA; Figure 8) using three groups of predictors: microenvironmental factors (slope degree, slope aspect, slope position, and microhabitat), plant structural factors (plant species and life forms), and plant nutrient factors (plant nutrient contents). Collectively, these factors explained 34.2% of the total variance in the soil stoichiometric dataset. Among them, microenvironmental factors exhibited the highest unique contribution (23.5%), while plant structural factors and plant nutrient factors showed considerably lower individual contributions (only 2.5% and 1.0%, respectively). Regarding interaction effects, the joint contributions of microenvironmental with plant nutrient factors (3.8%) and of microenvironmental with plant structural factors (2.1%) were both higher than that between the two plant-related factor groups (1.1%). Overall, the three-way interaction among all factor categories was minimal, explaining merely 0.2% of the variance.

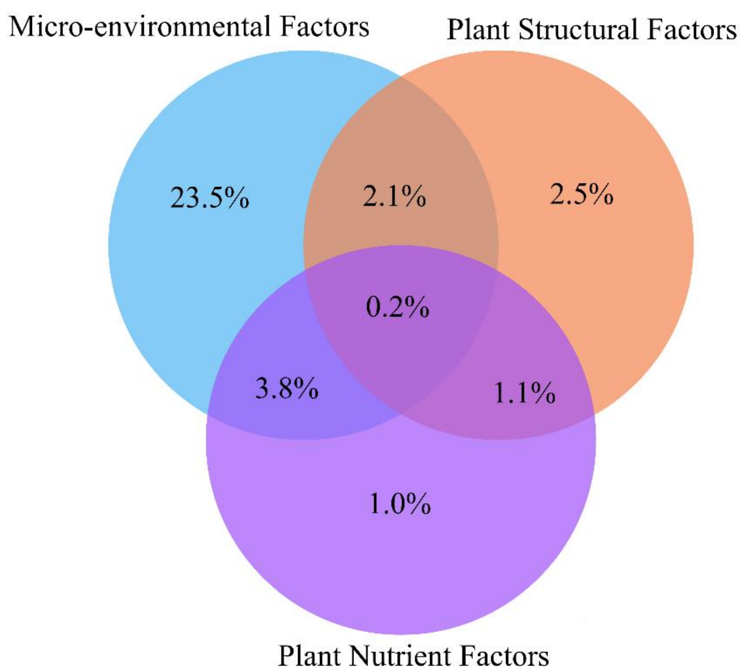

Figure 8. Variance partitioning analysis (VPA) of multi-factor contributions to soil stoichiometric characteristics. Tri-color overlapping system denotes environmental factor contributions: Blue: Microenvironmental factors (slope/aspect/position/microhabitat); Orange: Plant structural factors (species/life form); Purple: Plant nutrient factors (C/N/P/K/Ca/Mg contents); Values in overlapping areas indicate joint explanatory effects. Residuals = 65.8%.

4 Discussion

4.1 Stoichiometry-based nutrient cycling strategies in karst forest soils

This study found that the soil organic matter decomposition and nitrogen mineralization rates in the Maolan karst area were remarkably high, indicating a highly efficient internal nitrogen cycling within the ecosystem. This rapid nutrient turnover helps the ecosystem maintain its nitrogen supply, thereby alleviating nitrogen limitation pressure. This conclusion is supported by the relatively high overall contents of SOC and TN (125.08 and 11.20 g·kg^{-1}, respectively), coupled with a low mean SOC:TN ratio (10.83). This ratio is notably lower than the mean values for subtropical forest soils in China (14.88) (Qiao et al., 2020) and the global average (13.33) (Hessen et al., 2004), a phenomenon strikingly similar to observations from the Ibuki karst area in Japan (Kajino et al., 2023). Consistent with previous studies in semi-arid karst regions (e.g., Turkey), an SOC:TN ratio below 20 typically indicates strong microbial activity, suggesting that the rate of soil organic matter decomposition likely exceeds its accumulation rate (Dindaroglu et al., 2021). Consequently, we infer that the microbe-driven decomposition of organic matter and N mineralization proceed at a rapid pace, representing a “rapid carbon-nitrogen cycling” strategy adapted to fragmented habitats and shallow soils. Furthermore, the overall variation in the SOC:TN ratio was weak, indicating a relatively stable pattern. This stability may arise from the synchronous response of SOC and TN release and migration to environmental conditions (Feng et al., 2021). The formation of a relatively fixed ratio during microbial breakdown of organic matter aligns with other studies reporting a relatively stable soil SOC:TN ratio (Li et al., 2017).

Unlike nitrogen, we found that the intensity of phosphorus limitation in the study area was primarily influenced by microtopography-driven nutrient redistribution processes. Although the mean TP content reached 0.99 g kg^{-1}—approximately 2.61 times the average for subtropical evergreen broadleaf forests in China (0.38 g kg^{-1}) (Wang et al., 2021)—the mean SOC:TP ratio on upslope positions (326.58) was significantly higher than the global average (186) (Zhao et al., 2015). Furthermore, the TN:TP ratio on upslopes reached 22.91, significantly exceeding both the average for subtropical forest soils (12.43) (Qiao et al., 2020) and the global average (13.1) (Yu and Chi, 2020). Consequently, microorganisms and plants on upslopes likely face considerable phosphorus scarcity.

In fact, phosphorus limitation is not uncommon in karst regions; similar reports are frequently found in studies of other karst forests worldwide, such as those in Puerto Rico (Medina et al., 2017). This phenomenon may be related to the relatively weak adsorption and deposition of phosphorus by soil particles, making it more susceptible to loss through erosion processes such as raindrop splash and runoff (Di Palo and Fornara, 2017). Previous studies suggest that when the soil SOC:TP ratio exceeds 200, it indicates carbon abundance but phosphorus scarcity, potentially leading to microbial competition for limited phosphorus resources during decomposition (Qin et al., 2016). Excessively high TN:TP ratios may result in relatively lower biological nitrogen fixation, reducing the supply of available nitrogen (e.g., HN) (Yang et al., 2015). Similar phenomena have been observed in studies of the Bohemian Karst, where researchers suggested that phosphorus deficiency likely adversely affects soil nitrogen mineralization and reduces nutrient use efficiency in karst soils (Hofmeister et al., 2002).

Therefore, in response to pronounced phosphorus limitation, vegetation on upslopes in karst regions tends to adopt a conservative, defensive growth strategy, enhancing carbon accumulation capacity to improve stress tolerance. The nutrient return from the decomposition of fine roots, leaves, and other litter also contributes to the elevated SOC:TN and SOC:TP ratios in the soil (Dou et al., 2024).

Furthermore, this study found that the balance between soil calcium and magnesium (TCa:TMg) was significantly influenced by key biotic factors, such as surface plants. Specifically, the mean TCa:TMg ratio in soils associated with shrubs and herbs was generally greater, or significantly greater, than that in soils under tree life forms (evergreen and deciduous trees). However, there was almost no significant difference in TMg content among the different life forms. In terms of absolute element contents, TCa exhibited stronger variability within the study area, with its mean content (17.72 $g \cdot kg^{-1}$) being nearly three times that of TMg (6.51 $g \cdot kg^{-1}$), which indicates that fluctuations in TCa had a greater impact on the TCa:TMg ratio (Lu et al., 2014).

During sampling, we observed that shrubs and herbs growing densely on the ground surface intercepted and decomposed a substantial amount of litterfall from trees. The calcium released during this decomposition process may be subsequently replenished into the soil via rainfall (Schmitt et al., 2013). Studies in European karst regions have also indicated that increased soil Ca^{2+} content can alter the structure and abundance of soil bacterial communities and may contribute to the stabilization of soil organic matter (Pastore et al., 2022). This is because calcium plays a vital role in promoting the assimilation of other nutrient elements and stimulating microbial activity (Lukina et al., 2019). On one hand, calcium can react with soil organic matter to enhance its sequestration; on the other hand, it can stimulate the formation of soil micro-aggregates, thereby improving soil structure (Yang et al., 2023). Correspondingly, in this study, we found that the contents of major nutrients such as SOC, TN, and TP were relatively higher in areas dominated by shrubs and herbs. This life-form-mediated differentiation in soil stoichiometry reveals a ecological feedback: shrubs and herbs growing densely on the ground surface influence the distribution characteristics of soil nutrients in the rhizosphere zone by effectively intercepting and decomposing calcium-rich litterfall (including inputs from the tree canopy). Therefore, plants are not merely passive adapters to their environment but are also key active agents that shape the karst geochemical landscape through their life activities (Takahashi, 2021).

Although no significant differences in soil TMg content were observed among different plant life forms, we noted that the TMg content in herbaceous soils was generally lower, with a mean value only 78.06% to 83.78% of that in soils of other life forms. In contrast, the TN content in herbaceous soils was 1.22 to 1.60 times higher than that in other soils. This disparity resulted in a TN:TMg ratio in herbaceous soils that was greater than, or significantly greater than, that of other life forms. This pattern is consistent with findings from other studies indicating a negative correlation between soil nitrogen and magnesium. Specifically, when forest soil TN content is relatively high, the leaching of excess nitrate may be a key factor contributing to the reduction of soil magnesium content (Wang et al., 2022). Previous studies on coniferous forests in California, USA, have indicated that carbonate rocks are often rich in nitrogen, and their dissolution process can significantly increase ecosystem nitrogen content (Xiao et al., 2024). In our study area, herbaceous plants are typically distributed in downslope positions and depressions, where runoff convergence accelerates rock dissolution rates and consequently higher nitrogen release. Simultaneously, Ca^{2+} released during the dissolution process can facilitate nitrate leaching (Perakis et al., 2013). These combined mechanisms contribute to the relatively high TN:TMg ratio observed in soils associated with the herbaceous plant life form. Furthermore, other studies have also indicated that whether magnesium can promote plant growth appears to be significantly influenced by light conditions and the soil's nitrogen supply potential (Grzebisz, 2013). This is because Mg often plays a crucial role in enhancing plant nitrogen use efficiency (Wang et al., 2018), while also promoting photosynthesis, protein synthesis, and transport processes (Farhat et al., 2016). In this study, herbaceous plants generally grow in the understory, where they experience significant shading from trees and shrubs. Consequently, the relatively high soil TN:TMg ratio and limited light resources are likely to act as limiting factors for their growth.

4.2 Main driving factors of soil nutrient patterns in karst forests

This study reveals that the spatial heterogeneity of soil nutrients in the Maolan karst forest is not randomly distributed but rather forms an ordered pattern jointly shaped by key environmental factors such as microhabitat, microtopography, and plant life form (Peng and Dai, 2022). The combined regulation of these multiple factors on the input, migration, accumulation, and loss of soil nutrients constitutes a crucial driving mechanism for soil nutrient cycling in karst forests.

4.2.1 Microhabitat factors

This study identifies microhabitat as one of the dominant factors leading to the spatial heterogeneity of soil nutrients. It primarily influences the spatial redistribution of moisture and nutrients by affecting rock exposure rate and the intensity of material exchange at the soil-rock interface. Within the study area, most nutrients exhibited a distribution pattern of “enrichment on stone surfaces and depletion on soil surfaces.” For instance, the contents of major elements such as SOC and TN were significantly higher in stone surface microhabitats than in soil surface microhabitats ($P < 0.05$). This is likely related to the uneven distribution and poor connectivity of organic matter in the karst area. Stone surface microhabitats with high rock exposure may form relatively enclosed or semi-enclosed microenvironments due to bedrock barriers, facilitating surface water retention and litter accumulation, which ultimately transforms into humus. In contrast, soil surface microhabitats with low exposure rates lack surrounding rock barriers and have gentler slopes, resulting in relatively less organic matter, higher soil bulk density, and greater nutrient loss due to stronger leaching effects. Previous research on this phenomenon has indicated that the spatial heterogeneity of rock exposure significantly regulates the differentiation patterns of hydrological connectivity and material transport pathways, acting as a key environmental factor influencing soil structure formation and the biogeochemical cycling of major nutrient elements (Waring et al., 2020). Under the effects of rock dissolution and soil erosion, the surface becomes fragmented, increasing the difficulty of nutrient migration and leading to relatively stable stoichiometric characteristics within microhabitats (Jiang et al., 2014). Similar phenomena exist in other subtropical karst areas, where organic matter tends to accumulate richly in stone surface microhabitats, with indicators such as macro-aggregate content and mean weight diameter being relatively higher, and soil aggregate stability and nutrient content superior to those in soil surface microhabitats (Bi et al., 2024). Furthermore, the relatively better soil nutrient status can, in turn, improve the input conditions of soil nutrients by participating in the regulation of surface vegetation community structure, root growth, and litter dynamics, ultimately forming a positive feedback loop (Huang and Yuan, 2021).

It is important to note that the distribution of calcium in this study is related not only to nutrient segregation among microhabitats but also to its aggregation effect (Toko et al., 2017). Previous researchers have found that soil calcium in karst areas primarily originates from the weathering of soil-forming parent rocks. Its release, accumulation, and migration are often influenced by factors such as soil development, habitat topography, and soil acidity and alkalinity (Luo et al., 2023). When the soil is alkaline, ExCa binds more tightly to soil colloids. However, a decrease in soil pH can lead to easier exchange between ExCa on the colloids and H^+ ions, causing ExCa to detach from the colloids and enter the solution, where it is ultimately absorbed and utilized by plant roots or leached away. Consequently, the stone surface microhabitat, characterized by stronger weathering, higher pH, and a larger interfacial exchange area, may develop a distinct pattern of calcium ion release and accumulation compared to other microhabitats (Wei et al., 2018). More importantly, previous research on the Slovak karst region indicated that calcium ions in the soil serve not only as a nutrient element but also play a crucial role in the sequestration and stabilization of soil organic matter. This is because calcium ions can promote the aggregation and stabilization of organic matter by forming cation bridges between organic colloids. Additionally, they can form thin carbonate coatings on the surface of particulate organic matter, thereby providing physical protection for soil organic matter (Ahmed et al., 2012). Taken together with our observations that the pH, ExCa content, and soil organic carbon content were significantly higher on the stone surface than on the soil surface, we propose that the mechanisms described above may provide a plausible explanation (Han et al., 2019).

4.2.2 Microtopographic factors

This study found that microtopographic factors (slope degree, slope aspect, slope position) significantly influenced the spatial distribution patterns of numerous elements. The enrichment areas of certain elements often shared common conditions: a flat slope, a shady slope aspect, and an upslope position. Regarding slope degree, steeper slopes generally exhibited poorer soil moisture and nutrient characteristics, a phenomenon consistent with reports from karst areas in Kentucky, USA (McGraw et al., 2023). This pattern is likely because gravity is the key mechanism through which slope degree affects moisture and nutrient distribution in karst regions. On steeper slopes, the amount of material transported downslope is potentially larger, and the transport velocity is potentially faster (Patton et al., 2018). Similar phenomena have been observed in studies of karst regions such as Bodoquena in Brazil, where slope degree influences colluvial deposit distribution, microbial activity, and erosion intensity (Silva et al., 2017). Consequently, the input and output processes of soil nutrients can differ significantly across varying slope degrees. However, the distribution pattern of some elements, notably AP, was the opposite. The AP content on flat and gentle slopes was less than or significantly less than that on steep and sharp slopes. This may be because flat and gentle areas are more prone to seasonal waterlogging, leading to higher levels of free calcium carbonate in the soil. This carbonate can combine with phosphorus to form calcium phosphate salts, which are difficult for plants to absorb and utilize (Yang et al., 2015). A similar phenomenon has also been reported in the Yucatan karst region of Mexico (Campo, 2016).

The impact of slope aspect primarily originates from the heterogeneity of light distribution. In this study, we observed that low values of numerous soil nutrient elements were frequently concentrated on sunny slopes and semi-sunny slopes but were rarely found on other slope aspects. This may be attributed to the relatively abundant habitat resources on shady slopes, where lower water evaporation rates enhance soil erosion resistance and nutrient retention capacity to some extent, thereby providing a more favorable ecological niche for vegetation growth (Dai et al., 2023). Similar conclusions have been reported in studies on the Caspian Sea karst region (Smirnova and Gennadiev, 2017). In contrast, stronger illumination on sunny slopes and relatively dry soil conditions may restrict nutrient uptake by plant roots and also affect nutrient release and mineralization by limiting litter decomposition (Geroy et al., 2011). This aligns with findings from karst areas in Mexico (Campo, 2016). Similar nutrient distribution patterns have also been observed by other researchers in non-karst regions such as the Tibetan Plateau. They attribute this to habitat heterogeneity, which promotes the development of superior functional traits in vegetation and microbial communities on shady slopes, thereby enabling more timely and effective replenishment and maintenance of the soil nutrient pool (Zhang et al., 2022). Therefore, this study concludes that although factors such as cloud cover and vegetation can modulate solar radiation on slopes, slope aspect remains one of the dominant factors determining the spatial heterogeneity of light availability in karst areas. This spatial heterogeneity in radiation conditions directly leads to significant gradients in heat and moisture distribution across different slope aspects, ultimately exerting a profound influence on the coupling process between soil moisture and nutrients (Pelletier et al., 2018). This finding is consistent with the conclusions drawn by other researchers regarding the subtropical karst areas (Li et al., 2021).

At the overall slope scale, this study found that the contents of certain elements (e.g., SOC, TN, TCa, TMg) were significantly higher at the upslope position than at the midslope position. This phenomenon is likely attributable to the differentiation in soil stoichiometric characteristics among slope positions, caused by variations in erosion intensity and divergent vegetation growth strategies. Conventional studies on non-karst slopes often suggest that during runoff transport and erosion processes, the upslope areas typically act as a “net exporter” of moisture and nutrients. The exported water and nutrients ultimately converge in downslope areas or depressions. Consequently, upslope positions generally have thinner soil layers and poorer water and nutrient retention capacity, whereas lower slopes or depressions tend to have more abundant water resources and higher nutrient contents (Yu et al., 2020). However, in karst regions characterized by high rock exposure rates and extremely fragmented topography, the migration and accumulation patterns of some elements are not entirely consistent with those observed on conventional slopes, primarily due to the highly heterogeneous and unpredictable leakage pathways inherent to karst systems. Some researchers have reported similar phenomena in karst slopes in Guangxi, China, where nutrient contents were higher at upslope positions. They suggested that this pattern might be related to the specific processes of soil erosion occurrence on karst slopes and the complex mechanisms by which vegetation influences soil nutrients (Dou et al., 2024).

4.2.3 Plant life form factors

This study found that surface plant life forms, through their differential nutrient uptake and return strategies, led to a patterned enrichment of various nutrients in the soil of the rhizosphere zones associated with different life forms. This likely occurs because vegetation, while actively adapting to the surface environment, also participates in regulating the dynamics of soil stoichiometry through processes such as root activity, litter input, and decomposition (Zou et al., 2021). Variations in litter decomposition, in particular, may result in significant differences in the biochemical properties and structural composition of forest floor nutrient cycling—a phenomenon that has also been confirmed in investigations of karst ecosystems in the eastern Mediterranean region (Babur et al., 2022). In this study, we observed substantial differences in near-surface litter accumulation among different plant life forms on the karst slopes. Shrubs and herbs, due to their clustered growth form close to the ground, often intercept more litter. This intercepted material includes not only litter produced by the shrubs and herbs themselves but also a considerable amount of tree litter transported by wind or surface runoff. In contrast, trees, which have minimal branching near the base of their trunks, intercept relatively less litter compared to the understory shrubs and herbs that grow densely at ground level. This phenomenon has also been noted in other literature. For example, some researchers have observed that the understory vegetation layer can extensively intercept and regulate the spatial distribution pattern of litter, indicating that litter accumulation decreases as distance from the base of the understory plants increases (M. Dearden and A. Wardle, 2008). Other researchers suggest that the process of litter interception by the understory layer may alter its microenvironment (including light, moisture, soil, and microbial communities), thereby influencing its decomposition trajectory (He et al., 2013).

Additionally, this study observed a phenomenon in the karst region of southwestern China strikingly similar to that reported in Mexican karst areas: under conditions of thin surface soil layers, most tree species—except shallow-rooted herbaceous plants—tend to penetrate their root systems into deeper rock crevices to meet their demands for water and nutrients (Estrada-Medina et al., 2013). We suggest that this process may be accompanied by root-mediated redistribution of soil moisture and certain nutrients (such as potassium). Therefore, the relationship between different vegetation types and soil stoichiometric characteristics is not static. Overall, the root activities of surface plants and the nutrient return from litter on karst slopes do not necessarily affect exclusively their own rhizosphere soil. Various factors, including plant species, growth stage, community composition, rock barriers, and runoff scouring, may collectively exert direct or indirect comprehensive influences on the stoichiometric characteristics of slope soils. This complexity contributes to the intricate mechanisms by which plant-related factors influence soils on karst slopes (McGraw et al., 2023).

4.3 Specificity of karst forest soils and research limitations

In summary, this study reveals that the stoichiometric characteristics of soils in the Maolan karst forest are shaped by the complex interplay of microtopographic, microhabitat, and plant life form factors, resulting in a highly heterogeneous, mosaic-like distribution pattern. This pattern stems from the inherent specificity of the karst ecosystem, characterized by thin soil layers, high bedrock exposure rates, and an alkaline geochemical background determined by carbonate rock parent material. These underlying conditions profoundly alter and amplify the spatial heterogeneity of ecological processes. For instance, the strong segmentation effect of the bedrock not only exacerbates the local enrichment and loss of nutrients by influencing hydrological connectivity, but the intense weathering and dissolution processes of the bedrock release calcium ions that significantly influence regional nutrient cycling. This makes calcium a key element connecting the rock-soil-vegetation system, a process rarely encountered in non-karst regions.

It should be noted that the sampling strategy of this study was based on predefined discrete habitat stratifications. While this approach enhanced sampling feasibility within the complex karst terrain, such discretization may not fully capture continuous environmental gradients, thereby constituting an inherent limitation in characterizing microenvironmental heterogeneity and sampling design in such habitats. Therefore, future research should transcend this static stratification framework and commit to adopting continuous environmental gradient monitoring and high-resolution sampling strategies to overcome this limitation. This will better capture the complexity of karst ecosystems and facilitate a paradigm shift from discrete stratification to process-driven approaches.

5 Conclusions

The stoichiometric characteristics of soils in the karst region exhibit a certain degree of synergistic adaptation with factors such as microhabitat, microtopography, and surface plant life forms, and are closely related to some of these influencing factors. Across the entire study area, nutrient contents showed strong variability and significant spatial heterogeneity.

Microhabitat factors significantly influenced soil nutrient accumulation, establishing a basic pattern of "enrichment on stone surfaces and depletion on soil surfaces". Soil surface microhabitats exhibited nutrient-poor characteristics due to intense leaching, whereas stone surface microhabitats, owing to their unique soil-rock interface effects, became the primary enrichment zones for most nutrients. However, the influence of microhabitat variations was not entirely consistent for all elements, resulting in some elements and stoichiometric ratios displaying distribution trends opposite to others. This also reveals differences in the migration and transformation mechanisms among different elements.

Microtopographic factors, by regulating the transport and redistribution pathways of soil materials and energy, were not only significantly correlated with soil nutrient patterns but also played a dominant role in shaping the spatial distribution gradients of some nutrient elements. However, not all nutrient elements exhibited identical response mechanisms to these external influencing factors during this process. Coupled with the effects of differentiated nutrient regulation and uptake strategies among different plant life forms, these interactions collectively shaped the complex and variable spatial distribution patterns of soil nutrients in the karst region. Overall, the stoichiometric characteristics of soils in the study area were interactively shaped by factors such as microhabitat, microtopography, and plant life forms, with microhabitat and microtopography playing a dominant role. Although surface plant life forms exerted certain influences on most elements through processes like nutrient return and root activities, their overall impact was relatively weak. Moreover, the manifestation of their regulatory effects was often closely linked to microhabitat and microtopography factors. This synergistic interplay of multiple factors reflects, to some extent, the complexity of nutrient cycling mechanisms in karst soils.

Data availability. The data generated in this study are available from the first or corresponding author upon reasonable request.

Author contributions. Methodology, Data curation, Writing - review & editing, Writing - original draft, Visualization, Validation: YD. Investigation, Supervision: HZ. Formal analysis, Supervision: WZ. Investigation, Validation: YC. Conceptualization, Formal analysis: CT. Formal analysis, Investigation: FD. Formal analysis, Investigation: YW. Methodology, Supervision: RL. Funding acquisition, Visualization, Writing original draft, Writing - review & editing: PW.

Competing interests. The contact author has declared that none of the authors has any competing interests.

Financial support. This research was financially supported by the National Natural Science Foundation of China (32460275, 32060244).

References

Ahmed, Y. A., Pichler, V., Homolák, M., Gömöryová, E., Nagy, D., Pichlerová, M. and Gregor, J.: High organic carbon stock in a karstic soil of the Middle-European Forest Province persists after centuries-long agroforestry management, Eur. J. Forest Res., 131, 1669-1680, http://doi.org/10.1007/s10342-012-0608-7, 2012.

An, H., Tang, Z. S., Keesstra, S. and Shangguan, Z. P.: Impact of desertification on soil and plant nutrient stoichiometry in a desert grassland, Sci Rep-Uk, 9, 9422, http://doi.org/10.1038/s41598-019-45927-0, 2019.

Babur, E., Dindaroğlu, T., Riaz, M. and Uslu, O. S.: Seasonal Variations in Litter Layers' Characteristics Control Microbial Respiration and Microbial Carbon Utilization Under Mature Pine, Cedar, and Beech Forest Stands in the Eastern Mediterranean Karstic Ecosystems, Microb. Ecol., 84, 153-167, http://doi.org/10.1007/s00248-021-01842-4, 2022.

Bi, M. F., Zhang, S. P., Xu, Q. X., Hou, S. Z., Han, M. W. and Yu, X. R.: Coupling and synergistic relationships between soil aggregate stability and nutrient stoichiometric characteristics under different microtopographies on karst rocky desertification slopes, Catena, 243, 108142, http://doi.org/10.1016/j.catena.2024.108142, 2024.

Campo, J.: Shift from ecosystem P to N limitation at precipitation gradient in tropical dry forests at Yucatan, Mexico, Environ Res Lett, 11, 95006, http://doi.org/10.1088/1748-9326/11/9/095006, 2016.

Chen, Y., Li, Y. Q., Duan, Y. L., Wang, L. L., Wang, X. Y., Yao, C. P., Chen, Y. P., Cao, W. J. and Niu, Y. Y.: Patterns and driving factors of soil ecological stoichiometry in typical ecologically fragile areas of China, Catena, 219, 106628, http://doi.org/10.1016/j.catena.2022.106628, 2022.

Chen, Z. X., Xu, X., Wen, Y. L., Cheng, M. and Wang, X.: The critical role of soil ecological stoichiometric ratios: How does reforestation improve soil nitrogen and phosphorus availability? Plants, 13, 2320, http://doi.org/10.3390/plants13162320, 2024.

Dai, L. C., Fu, R. Y., Guo, X. W., Du, Y. G., Zhang, F. W. and Cao, G. M.: Variations in and factors controlling soil hydrological properties across different slope aspects in alpine meadows, J. Hydrol., 616, 128756, http://doi.org/10.1016/j.jhydrol.2022.128756, 2023.

Di Palo, F. and Fornara, D. A.: Plant and soil nutrient stoichiometry along primary ecological successions: Is there any link? Plos One, 12, e182569, http://doi.org/10.1371/journal.pone.0182569, 2017.

Dindaroglu, T., Babur, E., Battaglia, M., Seleiman, M., Uslu, O. S. and Roy, R.: Impact of Depression Areas and Land-Use Change in the Soil Organic Carbon and Total Nitrogen contents in a Semi-Arid Karst Ecosystem, Cerne, 27, 102980, http://doi.org/10.1590/01047760202127012980, 2021.

Dou, L., Zhang, W., Qin, M. E., Liang, Y. M. and Pan, F. J.: Seasonal variation of ecological stoichiometriccharacteristics of C,N and P in fine roots fromkarst forest and its influencing factors, Guihaia, 44, 452-464, http://doi.org/10.11931/guihaia.gxzw202210018, 2024.

Estrada-Medina, H., Graham, R. C., Allen, M. F., Jiménez-Osornio, J. J. and Robles-Casolco, S.: The importance of limestone bedrock and dissolution karst features on tree root distribution in northern Yucatán, México, Plant Soil, 362, 37-50, http://doi.org/10.1007/s11104-012-1175-x, 2013.

Farhat, N., Elkhouni, A., Zorrig, W., Smaoui, A., Abdelly, C. and Rabhi, M.: Effects of magnesium deficiency on photosynthesis and carbohydrate partitioning, Acta Physiol. Plant., 38, 145, http://doi.org/10.1007/s11738-016-2165-z, 2016.

Feng, M. D., Zhang, D. Y., He, B. H., Liang, K., Xi, P. D., Bi, Y. F., Huang, Y. Y., Liu, D. X. and Li, T. Y.: Characteristics of soil C, N, and P stoichiometry as affected by land use and slope position in the three gorges reservoir area, Southwest China, Sustainability-Basel, 13, 9845, http://doi.org/10.3390/su13179845, 2021.

Feng, W. L., Yang, J. L., Xu, L. G. and Zhang, G. L.: The spatial variations and driving factors of C, N, P stoichiometric characteristics of plant and soil in the terrestrial ecosystem, Sci. Total Environ., 951, 175543, http://doi.org/10.1016/j.scitotenv.2024.175543, 2024.

Geroy, I. J., Gribb, M. M., Marshall, H. P., Chandler, D. G., Benner, S. G. and McNamara, J. P.: Aspect influences on soil water retention and storage, Hydrol. Process., 25, 3836-3842, http://doi.org/10.1002/hyp.8281, 2011.

Grzebisz, W.: Crop response to magnesium fertilization as affected by nitrogen supply, Plant Soil, 368, 23-39, http://doi.org/10.1007/s11104-012-1574-z, 2013.

Han, J. J., Duan, X. and Zhao, Y. Y.: Spatial and temporal variability of soil moisture on slope land of different vegetation of dry-hot valley in Jinsha River, Arid Land Geography, 42, 121-129, http://doi.org/10.12118/j.issn.1000-6060.2019.01.14, 2019.

Han, T. F., Cai, A. D., Liu, K. L., Huang, J., Wang, B. R., Li, D. C., Qaswar, M., Feng, G. and Zhang, H. M.: The links between potassium availability and soil exchangeable calcium, magnesium, and aluminum are mediated by lime in acidic soil, J. Soil. Sediment., 19, 1382-1392, http://doi.org/10.1007/s11368-018-2145-6, 2019.

He, X. B., Lin, Y. H., Han, G. M. and Ma, T. W.: Litterfall interception by understorey vegetation delayed litter decomposition in Cinnamomum camphora plantation forest, Plant Soil, 372, 207-219, http://doi.org/10.1007/s11104-013-1734-9, 2013.

Hessen, D. O., Agren, G. I., Anderson, T. R., Elser, J. J. and De Ruiter, P. C.: Carbon, sequestration in ecosystems: The role of stoichiometry, Ecology, 85, 1179-1192, http://doi.org/10.1890/02-0251, 2004.

Hofmeister, J., Mihaljevič, M., Hošek, J. and Sádlo, J.: Eutrophication of deciduous forests in the Bohemian Karst (Czech Republic): the role of nitrogen and phosphorus, Forest Ecol. Manag., 169, 213-230, http://doi.org/10.1016/S0378-1127(01)00756-3, 2002.

Huang, J. and Yuan, Z. N.: Ecological stoichiometric characteristics of soil SOC, TN, and TP under different restoration methods in QiXing river wetland, Journal of King Saud University - Science, 33, 101407, http://doi.org/10.1016/j.jksus.2021.101407, 2021.

Jiang, Z. C., Lian, Y. Q. and Qin, X. Q.: Rocky desertification in Southwest China: Impacts, causes, and restoration, Earth-

Sci. Rev., 132, 1-12, http://doi.org/10.1016/j.earscirev.2014.01.005, 2014.

Joshi, R. K. and Garkoti, S. C.: Influence of vegetation types on soil physical and chemical properties, microbial biomass and stoichiometry in the central Himalaya, Catena, 222, 106835, http://doi.org/10.1016/j.catena.2022.106835, 2023.

Kajino, H., Fukui, M., Fujimoto, Y., Fujii, R., Yokobe, T., Tatsumi, C., Sugai, T., Okada, N. and Nakamura, R.: Variations in soil nutrient availabilities and foliar nutrient concentrations of trees between temperate monsoon karst and non-karst forest ecosystems on Mount Ibuki in Japan, Ecol. Res., 38, 842-851, http://doi.org/10.1111/1440-1703.12414, 2023.

Li, D. J., Wen, L., Zhang, W., Yang, L. Q., Xiao, K. C., Chen, H. and Wang, K. L.: Afforestation effects on soil organic carbon and nitrogen pools modulated by lithology, Forest Ecol. Manag., 400, 85-92, http://doi.org/10.1016/j.foreco.2017.05.050, 2017.

Li, T. Y., Zeng, J. M., He, B. H. and Chen, Z. P.: Changes in soil C, N, and P concentrations and stoichiometry in karst trough valley area under ecological restoration: the role of slope aspect, land use, and soil depth, Forests, 12, 144, http://doi.org/10.3390/f12020144, 2021.

Lu, X. K., Mao, Q. G., Gilliam, F. S., Luo, Y. Q. and Mo, J. M.: Nitrogen deposition contributes to soil acidification in tropical ecosystems, Global Change Biol., 20, 3790-3801, http://doi.org/10.1111/gcb.12665, 2014.

Lukina, N. V., Tikhonova, E. V., Danilova, M. A., Bakhmet, O. N., Kryshen, A. M., Tebenkova, D. N., Kuznetsova, A. I., Smirnov, V. E., Braslavskaya, T. Y., Gornov, A. V., Shashkov, M. P., Knyazeva, S. V., Kataev, A. D., Isaeva, L. G. and Zukert, N. V.: Associations between forest vegetation and the fertility of soil organic horizons in northwestern Russia, For Ecosyst, 6, 34, http://doi.org/10.1186/s40663-019-0190-2, 2019.

Luo, Y., Shi, C. M., Yang, S. T., Liu, Y., Zhao, S. and Zhang, C. C.: Characteristics of soil calcium content distribution in karst dry-hot valley and its influencing factors, Water-Sui, 15, 1119, http://doi.org/10.3390/w15061119, 2023.

M. Dearden, F. and A. Wardle, D.: The potential for forest canopy litterfall interception by a dense fern understorey, and the consequences for litter decomposition, Oikos, 117, 83-92, http://doi.org/10.1111/j.2007.0030-1299.16136.x, 2008.

McGraw, A., Ramsey, R. C., Obura, P., Matocha, C. and Shepard, C.: Topographic gradients of soil physical, chemical, and mineralogical properties in central Kentucky sinkholes, Soil Sci. Soc. Am. J., 87, 82-103, http://doi.org/10.1002/saj2.20478, 2023.

Medina, E., Cuevas, E. and Lugo, A.: Substrate Chemistry and Rainfall Regime Regulate Elemental Composition of Tree Leaves in Karst Forests, Forests, 8, 182, http://doi.org/10.3390/f8060182, 2017.

Nagamatsu, D., Hirabuki, Y. and Mochida, Y.: Influence of micro-landforms on forest structure, tree death and recruitment in a Japanese temperate mixed forest, Ecol. Res., 18, 533-547, http://doi.org/10.1046/j.1440-1703.2003.00576.x, 2003.

Pastore, G., Weig, A. R., Vazquez, E. and Spohn, M.: Weathering of calcareous bedrocks is strongly affected by the activity of soil microorganisms, Geoderma, 405, 115408, http://doi.org/10.1016/j.geoderma.2021.115408, 2022.

Patton, N. R., Lohse, K. A., Godsey, S. E., Crosby, B. T. and Seyfried, M. S.: Predicting soil thickness on soil mantled hillslopes, Nat Commun, 9, 3329, http://doi.org/10.1038/s41467-018-05743-y, 2018.

Pelletier, J. D., Barron Gafford, G. A., Gutiérrez Jurado, H., Hinckley, E. L. S., Istanbulluoglu, E., McGuire, L. A., Niu, G.

Y., Poulos, M. J., Rasmussen, C., Richardson, P., Swetnam, T. L. and Tucker, G. E.: Which way do you lean? Using slope aspect variations to understand Critical Zone processes and feedbacks, Earth Surf. Proc. Land., 43, 1133-1154, http://doi.org/10.1002/esp.4306, 2018.

Peng, X. D. and Dai, Q. H.: Drivers of soil erosion and subsurface loss by soil leakage during karst rocky desertification in SW China, International Soil and Water Conservation Research, 10, 217-227, http://doi.org/10.1016/j.iswcr.2021.10.001, 2022.

Perakis, S. S., Sinkhorn, E. R., Catricala, C. E., Bullen, T. D., Fitzpatrick, J. A., Hynicka, J. D. and Cromack, K.: Forest calcium depletion and biotic retention along a soil nitrogen gradient, Ecol. Appl., 23, 1947-1961, http://doi.org/10.1890/12-2204.1, 2013.

Qiao, Y., Wang, J., Liu, H. M., Huang, K., Yang, Q., Lu, R. L., Yan, L. M., Wang, X. H. and Xia, J. Y.: Depth-dependent soil C-N-P stoichiometry in a mature subtropical broadleaf forest, Geoderma, 370, 114357, http://doi.org/10.1016/j.geoderma.2020.114357, 2020.

Qin, J., Kong, H. Y. and Liu, H.: Stoichiometric characteristics of soil C,N,P and K indifferent *Pinus massoniana* forests, Journal of Northwest A&F University (Nat. Sci. Ed.), 44, 68-76, http://doi.org/10.13207/j.cnki.jnwafu.2016.02.010, 2016.

Sardans, J., Janssens, I. A., Ciais, P., Obersteiner, M. and Peñuelas, J.: Recent advances and future research in ecological stoichiometry, Perspectives in Plant Ecology, Evolution and Systematics, 50, 125611, http://doi.org/10.1016/j.ppees.2021.125611, 2021.

Schmitt, A., Cobert, F., Bourgeade, P., Ertlen, D., Labolle, F., Gangloff, S., Badot, P., Chabaux, F. and Stille, P.: Calcium isotope fractionation during plant growth under a limited nutrient supply, Geochim. Cosmochim. Ac., 110, 70-83, http://doi.org/10.1016/j.gca.2013.02.002, 2013.

Silva, M. B., Anjos, L. H. C. D., Pereira, M. G., Schiavo, J. A., Cooper, M. and Cavassani, R. D. S.: Soils in the karst landscape of Bodoquena plateau in cerrado region of Brazil, Catena, 154, 107-117, http://doi.org/10.1016/j.catena.2017.02.022, 2017.

Smirnova, M. A. and Gennadiev, A. N.: Quantitative assessment of pedodiversity and soil erosion within a karst sinkhole in the dry steppe subzone, Eurasian Soil Sci+, 50, 873-884, http://doi.org/10.1134/S1064229317080105, 2017.

Takahashi, M.: Nutrient storage and stoichiometry of the forest floor organic matter in Japanese forests, Soil Systems, 5, 51, http://doi.org/10.3390/soilsystems5030051, 2021.

Tang, J., Tang, X. X., Qin, Y. M., He, Q. S., Yi, Y. and Ji, Z. L.: Karst rocky desertification progress: Soil calcium as a possible driving force, Sci. Total Environ., 649, 1250-1259, http://doi.org/10.1016/j.scitotenv.2018.08.242, 2019.

Toko, T., Ito, Y., Sei, F., Michiru, Y., Akifumi, S., Takeo, M., Toru, O. and Yasuhiro, H.: Calcium is cycled tightly in Cryptomeria japonica stands on soils with low acid buffering capacity, Forest Ecol. Manag., 399, 64-73, http://doi.org/10.1016/j.foreco.2017.04.022, 2017.

Wang, J., Wen, X. F., Zhang, X. Y., Li, S. G. and Zhang, D. Y.: Co-regulation of photosynthetic capacity by nitrogen, phosphorus and magnesium in a subtropical Karst forest in China, Sci Rep-Uk, 8, 7406, http://doi.org/10.1038/s41598-

018-25839-1, 2018.

Wang, Q. W., Pieristè, M., Liu, C. G., Kenta, T., Robson, T. M. and Kurokawa, H.: The contribution of photodegradation to litter decomposition in a temperate forest gap and understorey, The New phytologist, 229, 2625-2636, http://doi.org/10.1111/nph.17022, 2021.

Wang, S. Q., Zhou, P. Y., Luo, B. and Ye, S. M.: Stoichiometric characteristics of medium- and micro-elements (Ca, Mg, Fe, and Mn) in soil aggregates as affected by stand age in Chinese fir plantations, Land Degrad. Dev., 33, 3991-4003, http://doi.org/10.1002/ldr.4439, 2022.

Waring, B. G., Sulman, B. N., Reed, S., Smith, A. P., Averill, C., Creamer, C. A., Cusack, D. F., Hall, S. J., Jastrow, J. D., Jilling, A., Kemner, K. M., Kleber, M., Liu, X. J. A., Pett Ridge, J. and Schulz, M.: From pools to flow: The PROMISE framework for new insights on soil carbon cycling in a changing world, Global Change Biol., 26, 6631-6643, http://doi.org/10.1111/gcb.15365, 2020.

Wei, X. C., Deng, X. W., Xiang, W. H., Lei, P. F., Ouyang, S., Wen, H. F. and Chen, L.: Calcium content and high calcium adaptation of plants in karst areas of southwestern Hunan, China, Biogeosciences, 15, 2991-3002, http://doi.org/10.5194/bg-15-2991-2018, 2018.

Wen, P. Y. and Jin, G. Z.: Effects of topography on species diversity in a typical mixed broadleaved-Korean pine forest, Acta Ecologica Sinica, 39, 945-956, http://doi.org/10.5846/stxb201801110086, 2019.

Wu, P., Zhou, H., Zhao, W. J., Yang, G. N., Cui, Y. C., Hou, Y. J., Tan, C. J., Zhou, T. and Ding, F. J.: Stoichiometric characteristics and influencing factors of different components of karst forest plants at the microtopography and microhabitat scale in Maolan National Nature Reserve, Guizhou, China, Forests, 16, 317, http://doi.org/10.3390/f16020317, 2025.

Xiao, D., Tang, Y. X., Zhang, W., Hu, P. L. and Wang, K. L.: Lithology and niche habitat have significant effect on arbuscular mycorrhizal fungal abundance and their interspecific interactions, Sci. Total Environ., 919, 170774, http://doi.org/10.1016/j.scitotenv.2024.170774, 2024.

Yang, H., Tu, C. Y., Li, Q. F., Yang, L. C. and Cao, J. H.: Analysis of C, N and P stoichiometry of secondary forest in different landforms in karst area, Journal of Southern Agriculture, 46, 777-781, http://doi.org/10.3969/j: issn.2095-1191.2015.5.777, 2015.

Yang, S., Yang, L., Wen, D., Liu, L., Ni, K., Cao, J., Zhu, T. and Müller, C.: Soil calcium constrains nitrogen mineralization and nitrification rates in subtropical karst regions, Soil Biology and Biochemistry, 186, 109176, http://doi.org/10.1016/j.soilbio.2023.109176, 2023.

Yang, Y. C. and Da, L. J.: A brief review of studies on differentiation of vegetation pattern along a topographic gradient in hilly regions, J. Plant Ecol, 30, 504-513, 2006.

Yu, H. Y., Zha, T. G., Zhang, X. X., Nie, L. S., Ma, L. M. and Pan, Y. W.: Spatial distribution of soil organic carbon may be predominantly regulated by topography in a small revegetated watershed, Catena, 188, 104459, http://doi.org/10.1016/j.catena.2020.104459, 2020.

Yu, Y. H. and Chi, Y. K.: Ecological Stoichiometric Characteristics of Soil at Different Depths in a Karst Plateau Mountain Area of China, Pol. J. Environ. Stud., 29, 969-978, http://doi.org/10.15244/pjoes/102781, 2020.

Zhang, C., Zeng, F. P., Zeng, Z. X., Du, H., Zhang, L. J., Su, L., Lu, M. Z. and Zhang, H.: Carbon, Nitrogen and Phosphorus stoichiometry and its influencing factors in karst primary forest, Forests, 13, 1990, http://doi.org/10.3390/f13121990, 2022.

Zhang, Q. P., Fang, R. Y., Deng, C. Y., Zhao, H. J., Shen, M. H. and Wang, Q.: Slope aspect effects on plant community characteristics and soil properties of alpine meadows on Eastern Qinghai-Tibetan plateau, Ecol. Indic., 143, 109400, http://doi.org/10.1016/j.ecolind.2022.109400, 2022.

Zhang, Y. L., Liu, M., Li, H., Yang, J. H., Zhao, X. Y., Qu, J. H., Li, L. J., Bai, Y. L., Yan, D. and Hou, G. N.: Spatial distribution characteristics of soil C:N:P:K eco-stoichiometry of farmland and grassland in the agro-pastoral ecotone in Inner Mongolia, China, Agronomy, 14, 346, http://doi.org/10.3390/agronomy14020346, 2024.

Zhao, F. Z., Sun, J., Ren, C. J., Kang, D., Deng, J., Han, X. H., Yang, G. H., Feng, Y. Z. and Ren, G. X.: Land use change influences soil C, N and P stoichiometry under 'Grain-to-Green Program' in China, Sci Rep-Uk, 5, 10195, http://doi.org/10.1038/srep10195, 2015.

Zhou, T., Cui, Y. C., Ye, Y. Y., Zhao, W. J., Hou, Y. J., Wu, P. and Ding, F.: Leaf functional traits of typical karst forest plants under different niches, Journal of Central South University of Forestry & Technology, 42, 129-140, http://doi.org/10.14067/j.cnki.1673-923x.2022.10.015, 2022.

Zou, Z. G., Zeng, F. P., Zeng, Z. X., Du, H., Tang, H. and Zhang, H.: The Variation in the Stoichiometric Characteristics of the Leaves and Roots of Karst Shrubs, Forests, 12, 852, http://doi.org/10.3390/f12070852, 2021.